Theory of spatial optical solitons in metallic nanowire materials

Mário G. Silveirinha*

University of Coimbra, Department of Electrical Engineering—Instituto de Telecomunicações, Portugal

(Received 30 March 2013; revised manuscript received 25 May 2013; published 12 June 2013)

I characterize the spatial optical solitons supported by arrays of metallic nanowires embedded in Kerr-type material. The array of nanowires is described using an effective medium model and is regarded as a continuous medium. I show that the conditions necessary for the formation of spatial solitons are radically different in presence of the nanowires. In particular, within the effective medium model, spatial solitons are allowed in the nanowire material only when the host material is a "self-defocusing" material. It is proven that the characteristic soliton beamwidth is related to the degree of hyperbolicity of the isofrequency surfaces of the photonic states and that a sufficiently strong electric field amplitude may enable subwavelength solitary waves.

DOI: 10.1103/PhysRevB.87.235115 PACS number(s): 42.70.Qs, 78.67.Pt, 42.65.−k, 41.20.Jb

I. INTRODUCTION

Light propagation in nanowire arrays has been a topic of intense research in recent years due to the opportunity provided by such structures to manipulate electromagnetic radiation on a spatial scale much smaller than the wavelength.[1–4] More recently, the impact of nonlinear effects[5,6] in light propagation in metallic nanowire arrays and other closely related nanostructures has been investigated.[7–13] It has been predicted that such "plasmonic waveguide arrays" may support subwavelength spatial solitons when the metallic inclusions are embedded in a nonlinear Kerr-type dielectric host.[7,8] This may enable achievement of the subwavelength confinement of light guided by metallic nanostructures and help reduce the characteristic size of photonic devices. Several studies have demonstrated that spatial solitons (also known as plasmonic lattice solitons) in nanowire arrays are stable when the nanowires are embedded in a self-defocusing medium,[7,8] and a variety of vortex and multipole have been studied in Refs. 14 and 15. The analysis of these works is based on the coupled-mode theory, which provides limited physical insight to the problem. Recently,[16] building on the efforts reported in several earlier papers,[17–19] I developed an effective medium model for regarding the array of metallic nanowires embedded in a Kerr-type material as a continuous medium characterized by some nonlinear effective parameters. It was shown that the nanowire array may behave as a hyperbolic (indefinite) uniaxial medium (such that the signs of the components of the permittivity tensor differ) and that a weak nonlinearity enables control of the degree of hyperbolicity of the dispersion of the photonic states. In particular, it was predicted that the nonlinear effects may enhance the negative refraction of light at an interface between air and nanowire array. In this paper, I apply the effective medium model to the study of spatial solitons in nanowire arrays embedded in a nonlinear host. Based on the effective medium framework, I explain the mechanism of formation of the spatial solitons. I prove that the interplay between the nonlinearity of the host and the wave-guiding properties of the plasmonic inclusions results in an effective medium response such that if the host dielectric (i.e., the nonlinear component of the composite material) is a self-defocusing medium, then the array of nanowires behaves as a self-focusing medium. I develop an analytical theory to characterize the spatial solitons and present a parametric numerical study of the properties of the spatial solitons in simple, two-dimensional scenarios, including the effect of loss.

II. TRAPPED STATES IN NONLINEAR HYPERBOLIC MEDIA

In this section, I discuss from a qualitative point of view the physical requirements for the formation of trapped states in arrays of metallic nanowires embedded in a nonlinear host medium with a Kerr-type nonlinearity. The array of nanowires is treated as an effective medium, and to a rough approximation, it may be regarded as a hyperbolic medium. This is because the isofrequency diagrams of the photonic states associated with the so-called quasitransverse electromagnetic (quasi-TEM) are hyperbolic contours.[18,20] As discussed in detail in my previous paper,[16] the shape of the isofrequency diagrams depends on the nonlinear effects and thus on the intensity of the electromagnetic field. Hyperbolic metamaterials have recently received considerable attention due to their applications in negative refraction of light[21] and in the enhancement of the Purcell factor,[22–24] among others.

The geometry of the nanowire array is illustrated in Fig. 1. It is assumed that the metallic nanowires are cylindrical, are oriented along the z direction, and have the radius r_w. The metal electric permittivity is ε_m. The period of the array is a. The nanowires are embedded in a host medium with a Kerr-type nonlinearity such that $\varepsilon_h = \varepsilon_h^0(1+\delta\varepsilon)$ with $\delta\varepsilon = \alpha\mathbf{e}^*\cdot\mathbf{e}$, where $\mathbf{e}$ is the microscopic electric field (i.e., before any averaging on the scale of the period of the array) and $\alpha = 3\chi^{(3)}/\varepsilon_{h,r}^0$ is a constant that determines the strength of the nonlinear effects.

The mechanism of formation of trapped states in conventional self-focusing media is well known and can be understood from the dynamics of the isofrequency contours of the photonic states as a function of the nonlinear effects. Suppose that the direction of propagation is along z and that k_{z0} is the wave number that determines the variation in space of the trapped state along the direction of propagation. For a fixed frequency, a trapped state associated with certain k_{z0} is allowed if the medium supports a photonic state with $k_z = k_{z0}$ (such that a generic photonic state is characterized by the wave vector $\mathbf{k} = \mathbf{k}_t + k_z\hat{\mathbf{z}}$, where $\mathbf{k}_t = k_x\hat{\mathbf{x}} + k_y\hat{\mathbf{y}}$) for a sufficiently strong field amplitude and simultaneously there

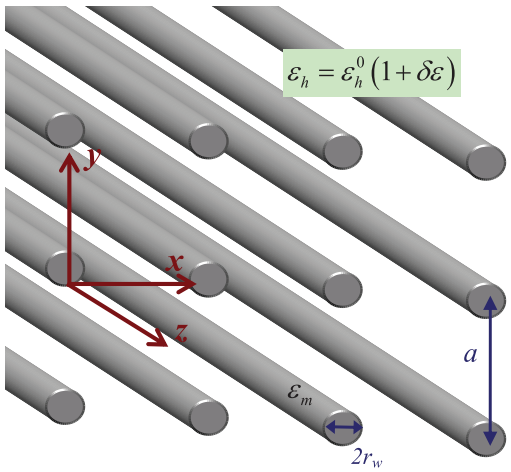

FIG. 1. (Color online) A periodic metallic nanowire array embedded in a Kerr-type nonlinear host material.

are no allowed photonic states with $k_z = k_{z0}$ for weak field amplitudes. In such circumstances, the radiation can become trapped for sufficiently strong field amplitudes because it cannot be coupled to photonic states lying in the regions of weak field amplitude. Thus, the trapping mechanism is related to the total-internal reflection due to the self-induced refractive index change.

These ideas are illustrated in Fig. 2(a), which shows the dispersion of the photonic states $k^2c^2 = \omega^2 n^2$ (c is the speed of light in vacuum) for a conventional self-focusing medium such that index of refraction n grows with the amplitude of the electric field. In Fig. 2(a), the dotted (green) line intersects the surface of allowed photonic states in case of a strong field amplitude (dashed yellow circle) but does not intersect the surface of allowed photonic states for low field amplitudes (solid blue circle).

In order to study when solitary waves are allowed in a nanowire material, I depict in Fig. 2(c) the isofrequency contours of the quasi-TEM mode in a case of weak fields at 1550 nm for a representative material geometry (solid black line). It is assumed that the nanowires are made of silver. The dispersion of silver is described by the Drude permittivity model with a plasma frequency 2175 THz.[25] As seen, the isofrequency surface of the photonic states resembles a hyperbola, rather different from what happens in a vacuum, where it is a spherical surface. In case the nanowires are embedded in a nonlinear material, the isofrequency contours depend on the effective parameters $n_{ef,h}^2$ and n_w^2/ζ_w, whose precise definition is given in Ref. 16 (see also Sec. III). When the nanowires are embedded in a self-focusing (self-defocusing) nonlinear material, $n_{ef,h}^2$ and n_w^2/ζ_w are greater (smaller) than unity and grow (become smaller) as the amplitude of the fields grows. For very weak fields (linear approximation), $n_{ef,h}^2 = n_w^2/\zeta_w = 1$. The perturbation in the dispersion of the photonic states caused by the nonlinear effects is represented in Fig. 2(c) with dashed green and dot-dashed blue lines for the cases of self-defocusing and self-focusing host medium, respectively.

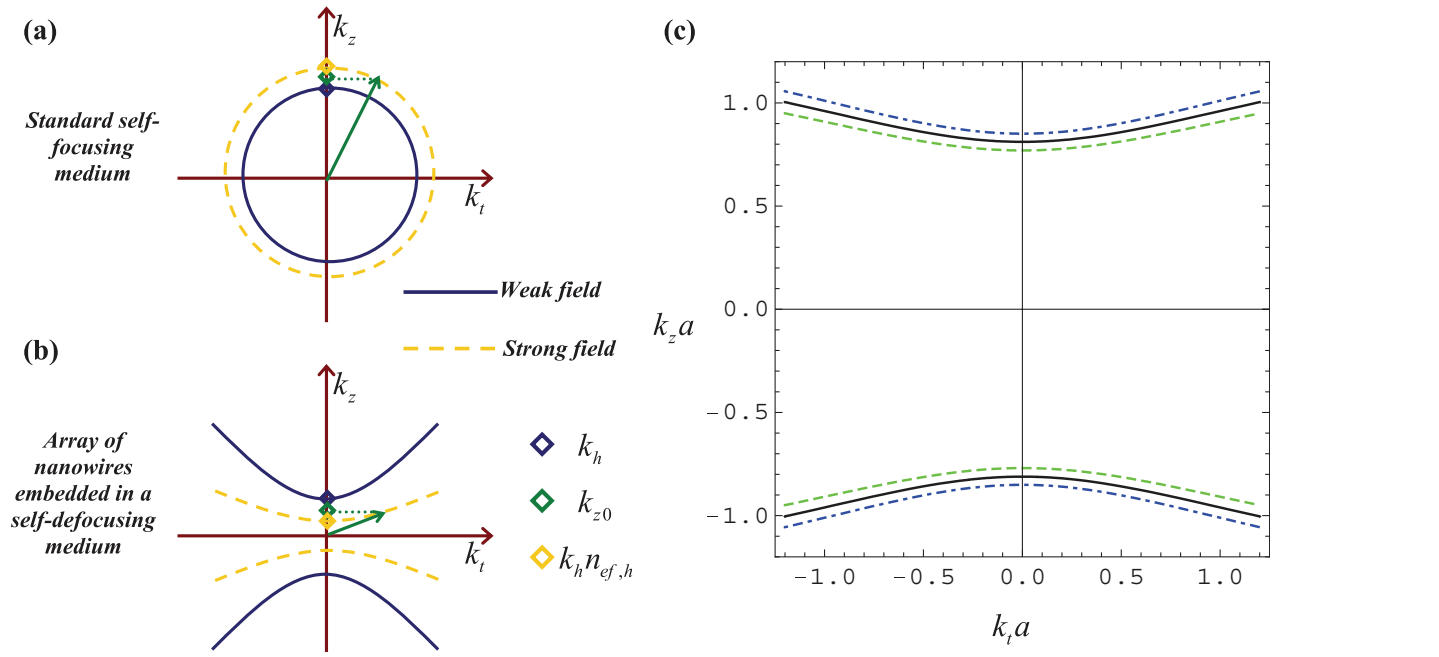

FIG. 2. (Color online) The mechanism that enables the formation of spatial solitons. (a) Dispersion of photonic states in a standard self-focusing medium for the cases of weak (solid blue line) and strong (dashed yellow line) field amplitudes. (b) Similar to (a) but for an array of nanowires embedded in a self-defocusing medium. (c) Dispersion of the photonic states associated with the extraordinary (quasi-TEM) wave at λ_0=1550 nm in a nanowire material formed by silver wires in a dielectric background with $\varepsilon_h^0 = 1.0\varepsilon_0$, $r_w = 20$ nm, and $r_w/a = 0.1$. The dispersion of the photonic states is obtained based on the theory of Ref. 16. Solid (black) lines are $n_{ef,h}^2 = n_w^2/\zeta_w = 1.0$ (linear host material), dot-dashed (blue) lines are $n_{ef,h}^2 = n_w^2/\zeta_w = 1.0 + 0.1$ (self-focusing host material); and dashed (green) lines are $n_{ef,h}^2 = n_w^2/\zeta_w = 1.0 - 0.1$ (self-defocusing host material). The green arrow in (a) and (b) represents a photonic state with $k_z = k_{z0}$ such that it only propagates in case of a sufficiently strong field.

It can be checked based on the analytical model of Ref. 16 that the vertex of the hyperbola (point of the hyperbola with $k_t = 0$) is such that $k_z = k_h n_{ef,h}$, where $k_h = \omega\sqrt{\varepsilon_h^0 \mu_0}$ and ε_h^0 is the permittivity of the host medium for the case of weak field amplitudes. Hence, based on this result and on the isofrequency contours of Fig. 2(c), we can readily understand in which circumstances trapped states can be formed in the effective medium. Taking into account the hyperbolic shape of the isofrequency surfaces, it is seen that the value k_{z0} associated with a trapped state must be such that (i) $k_{z0} > k_h n_{ef,h}$ so that a photonic state is allowed in the case of a sufficiently strong field amplitude (i.e., so that the dashed horizontal green line in Fig. 2(b) intersects the dashed yellow hyperbola) and (ii) $k_{z0} < k_h$ so that no photonic states are supported in the case of a weak field (i.e., so that the dashed horizontal green line in Fig. 2(b) does not intersect the solid blue hyperbola). The two conditions can be met simultaneously only if $n_{ef,h} < 1$, i.e., only in the case of a self-defocusing host medium. In particular, I conclude that within the effective medium model adopted here, no solitary waves are allowed in the nanowire material in the case of a self-focusing host medium. Figure 2(b) illustrates the isofrequency contours in a nanowire material with a self-defocusing host, and an allowed value for k_{z0} is marked on the plot.

Ref. 8 reported that discrete spatial solitons may be supported by arrays of metallic nanowires embedded in a Kerr self-focusing medium, in apparent contradiction with my theory. However, the two theories can be reconciled because for a self-focusing medium, the trapped states found in Ref. 8 are staggered solitons. Such trapped modes have strong spatial field variations on the scale of the period of the nanowire material and thus cannot be described within an effective medium approach, which is the scope of my paper.

The trapped waves described previously are partly related to gap solitons,[10–13,26,27] because the dispersion of the photonic states in the nanowire array has a directional band gap. However, here the spatial soliton formation does not involve Bragg scattering and is rooted on the effective medium response. The emergence of gap solitons in metamaterials has been discussed, for example, in Refs. 12 and 28.

III. EFFECTIVE MEDIUM MODEL FOR THE CHARACTERIZATION OF THE SPATIAL SOLITONS

In order to put the ideas of the previous section in a firm theoretical standing, I next derive the equations that allow calculating the spatial solitons in the nanowire material. The analysis is based on the effective medium model derived in Ref. 16, which describes the electrodynamics of the wire medium in terms of the state vector $(\mathbf{E},\mathbf{H},\varphi_w,I)$, where $(\mathbf{E},\mathbf{H})$ are the macroscopic electromagnetic fields, I is the current in the nanowires, and φ_w is the average quasistatic electric potential drop from a given nanowire to the boundary of the respective unit cell. Both I and φ_w are continuous functions of the position, so the wire array is regarded as a continuous medium. The state vector $(\mathbf{E},\mathbf{H},\varphi_w,I)$ satisfies a nonlinear first-order partial-differential system. However, it is possible to eliminate $(\mathbf{H},I)$ in favor of $(\mathbf{E},\varphi_w)$. This yields the following second-order partial-differential system (Ref. 16, Eq. 36):

$$\nabla\times\nabla\times\mathbf{E} - k_h^2 n_{ef,h}^2\mathbf{E} = i\omega\mu_0\mathbf{j}_{\rm ext} + \frac{\beta_p^2}{\zeta_w}\left(\frac{\partial\varphi_w}{\partial z} - E_z\right)\hat{\mathbf{z}} + \beta_p^2 k_h^2\tilde{\mathbf{Y}}\varphi_w, \tag{1a}$$

$$\frac{\partial^2\varphi_w}{\partial z^2} + k_h^2 n_w^2\varphi_w = -\zeta_w k_h^2\tilde{\mathbf{Y}}\cdot\mathbf{E}_t + \frac{\partial E_z}{\partial z}. \tag{1b}$$

where $k_h^2 = \omega^2\varepsilon_h^0\mu_0$, $\mathbf{E}_t = E_x\hat{\mathbf{x}} + E_y\hat{\mathbf{y}}$ is the transverse electric field component, $\mathbf{j}_{\rm ext}$ is a macroscopic current density that models external sources of radiation (in this paper $\mathbf{j}_{\rm ext} = 0$), $\zeta_w = 1 + \frac{Z_w}{-i\omega L}$, $Z_w = -\frac{1}{i\omega\pi r_w^2(\varepsilon_m - \varepsilon_h^0)}$ is the per unit of length (p.u.l.) self-impedance of the nanowires, $L = \frac{\mu_0}{2\pi}\log(\frac{a^2}{4r_w(a-r_w)})$ is the p.u.l. geometrical inductance of the nanowires, and $\beta_p = a^{-1}\sqrt{\mu_0/L}$ is the geometrical component of the effective plasma-wave number of the metamaterial.[19]

As a consequence of the nonlinear response of the host medium (described by the parameter α), the effective parameters $\tilde{\mathbf{Y}} = \frac{\alpha}{2}(\varphi_w\mathbf{E}_t^* + \varphi_w^*\mathbf{E}_t)$, $n_{ef,h}^2 = 1 + \alpha(\mathbf{E}^*\cdot\mathbf{E} + \beta_p^2\varphi_w\varphi_w^*)$, and $n_w^2 = \zeta_w[1 + \alpha(\mathbf{E}^*\cdot\mathbf{E} + \tilde{B}\,\beta_p^2\varphi_w\varphi_w^*)]$ are quadratic forms of the state vector. The dimensionless parameter $\tilde{B}$ depends exclusively on the normalized radius of the nanowires, r_w/a. An explicit formula for $\tilde{B}$ can be found in Ref. 16. The system of equations in Eq. (1) is the starting point for the calculation of the spatial solitons supported by the nanowire array based on the effective model.

To make further progress, it is necessary to simplify somewhat the system in Eq. (1). I consider two approaches based on different simplifications of the formulas for $n_{ef,h}^2$, n_w^2, and $\tilde{\mathbf{Y}}$. The parameters $n_{ef,h}^2$ and n_w^2 depend on $|E_z|^2$, $|E_t|^2$, and $|\varphi_w|^2$, with $|E_t| = \sqrt{|E_x|^2 + |E_y|^2}$. In the case of paraxial spatial solitons propagating along the z direction, the light beam is expected to be a quasiplane wave that barely penetrates into the metallic nanowires; thus, the associated electric field is mainly confined to the xoy plane so that $|E_z| \ll |E_t|$. Moreover, because φ_w is the quasistatic electric potential created by the electric charge density induced on the metallic wires,[16] for paraxial propagation we may also expect that $|\varphi_w/a| \ll |E_t|$. This will be confirmed later with numerical simulations. Hence, in the paraxial case, we can neglect contributions to the nonlinear dynamics arising from both E_z and φ_w. Thus, we may assume that

$$n_{ef,h}^2 \approx \frac{n_w^2}{\zeta_w} \approx 1 + \alpha\mathbf{E}_t^*\cdot\mathbf{E}_t, \quad \text{and} \quad \tilde{\mathbf{Y}} \approx 0. \tag{2}$$

With these approximations, the nonlinear system in Eq. (1) is considerably simplified:

$$\nabla\times\nabla\times\mathbf{E} - k_h^2 n_{ef,h}^2\mathbf{E} = i\omega\mu_0\mathbf{j}_{\rm ext} + \frac{\beta_p^2}{\zeta_w}\left(\frac{\partial\varphi_w}{\partial z} - E_z\right)\hat{\mathbf{z}}, \tag{3a}$$

$$\frac{\partial^2\varphi_w}{\partial z^2} + k_h^2\zeta_w n_{ef,h}^2\varphi_w = \frac{\partial E_z}{\partial z}. \tag{3b}$$

In this approach, I retain E_z and φ_w because they are necessary to couple the two second-order equations. The double curl operator could be further simplified using

the paraxial approximation, but this is not required unless someone is interested in studying the effect of perturbations (e.g., loss) in the propagation (see Sec. V).

The other approach considered here is based on a less drastic simplification of the effective medium model. As detailed in Appendix A, in this second approach, only the contribution from $|E_z|^2$ to the nonlinear dynamics is discarded so that $n_{ef,h}^2$ and n_w^2 are given by Eqs. (A1a) and (A1b), respectively, and the exact form of $\tilde{\mathbf{Y}}$ is retained. The neglect of $|E_z|^2$ is justified, because even in the nonparaxial case, we may expect $|E_z| \ll |E_t|$. It is known that in wire media formed by metals with high conductivity, the extraordinary wave remains a quasi-TEM with $|E_z| \ll |E_t|$, even when the fields vary appreciably along the x and y directions.[17–19] This is especially accurate when the radius of the wires is at least few times larger than the metal skin depth.

To determine the spatial solitons, we can solve either Eq. (3) (paraxial approach) or Eq. (1) (nonparaxial approach), assuming that the dependence on z of $(\mathbf{E},\varphi_w)$ is of the form $e^{ik_z z}$. For simplicity, I only consider two-dimensional solitary waves with $E_x = 0$ and $\partial_x = 0$. Moreover, for the reasons explained in Appendix A, we are interested in spatial solitons such that E_y and φ_w are in phase and E_y and E_z are in quadrature. Thus, we may look for solutions such that $E_y = \tilde{E}_y(y)e^{ik_z z}$ and $\varphi_w = \tilde{\varphi}_w(y)e^{ik_z z}$ with the respective envelopes $\tilde{E}_y$ and $\tilde{\varphi}_w$ real valued. It is proven in the Appendix A that within the paraxial approximation (Eqs. (2) and (3)) E_y and φ_w satisfy

$$\frac{\partial \varphi_w}{\partial y} = -\frac{k_z^2 - k_h^2 n_{ef,h}^2}{k_h^2 \zeta_w \left(n_{ef,h}^2 + \alpha E_y E_y^*\right) - k_z^2} E_y, \tag{4a}$$

$$\frac{\partial E_y}{\partial y} = -\frac{k_h^2 \zeta_w n_{ef,h}^2 - k_z^2 - \beta_p^2}{n_{ef,h}^2 + 2\alpha E_y E_y^*} n_{ef,h}^2 \varphi_w, \tag{4b}$$

where $n_{ef,h}^2$ is given by Eq. (2). In the more general nonparaxial approach [Eqs. (1) and (A1)], the fields E_y and φ_w satisfy a similar but more complex first-order nonlinear system [Eq. (A4)]. We restrict attention to solitons such that $\tilde{E}_y(y)$ is an even function of y; consequently, $\tilde{E}_z(y)$ and $\tilde{\varphi}_w(y)$ are odd functions of y. Thus, the boundary conditions at $y = 0$ are such that

$$\varphi_w|_{y=0} = 0 \quad \tilde{E}_y|_{y=0} = \tilde{E}_{y0} \tag{5}$$

The value of $\tilde{E}_{y0}$ depends on k_z and is determined iteratively in order to ensure that for $y \to +\infty$ the electromagnetic fields vanish: $E_y, \varphi_w \to 0$.

In the case of perfectly electric conducting (PEC) metallic wires, the normalized impedance ζ_w is equal to the unity. In such a case and for a linear host ($n_{ef,h}^2 = n_w^2/\zeta_w = 1$ and $\tilde{\mathbf{Y}} = 0$), it can be verified that when $k_z = k_h$, Eq. (1) admits a solution with $E_z = 0$ (TEM wave beam). Indeed, for $k_z = k_h$ and $E_z = 0$, Eq. (1b) is satisfied for an arbitrary envelope $\tilde{\varphi}_w(y)$ of the additional potential ($\varphi_w = \tilde{\varphi}_w(y)e^{ik_z z}$), whereas Eq. (1a) is satisfied with $\mathbf{E} = E_y \hat{\mathbf{y}}$ provided that

$$\frac{\partial E_y}{\partial y} = \beta_p^2 \varphi_w. \tag{6}$$

Thus, provided the envelope $\tilde{\varphi}_w(y)$ is chosen such that $\int_{-\infty}^{+\infty} \tilde{\varphi}_w(u)du = 0$ (e.g., any odd function localized in the vicinity of the origin), it follows that the corresponding wave beam, characterized by the envelope $\tilde{E}_y = \beta_p^2 \int_{-\infty}^{y} \tilde{\varphi}_w(u)du$, is also localized in space and propagates along the z direction with no diffraction, even though the host material is assumed to be linear. Thus, the PEC wire medium supports nondiffracting waves even in the limit of a linear response. This property is a consequence of the diffractionless nature of TEM waves in PEC wire media and of the effective medium being characterized by extreme anisotropy, as widely discussed in the literature.[17,18,29]

IV. NUMERICAL RESULTS

As a first example of the application of the theory of the previous section, Fig. 3 plots the normalized field profiles associated with a spatial soliton with $k_z = 0.990k_h$ at λ_0=1550 nm in an array of silver nanowires embedded in a self-defocusing host medium. It is supposed that the radius of the nanowires is $r_w = 20$ nm and that the period is $a = 200$ nm. The effect of dielectric and metallic loss is neglected here but is discussed in detail in the next section. It can be checked that the electric field and additional potential profiles associated with a given spatial soliton depend on the specific value of the nonlinear parameter ($\alpha < 0$) as $1/\sqrt{|\alpha|}$. For this reason, the field profiles in Fig. 3 are given in normalized unities. Without loss of generality, the permittivity of the host medium for weak field amplitudes is taken to be equal to the permittivity of vacuum $\varepsilon_h^0 = 1.0\varepsilon_0$. The results remain qualitatively similar in the more realistic situation $\varepsilon_h^0 > \varepsilon_0$. As seen in Fig. 3, the spatial soliton is a quasi-TEM beam, with $|E_z| \ll |E_t|$ and $|\varphi_w/a| \ll |E_t|$. The dot-dashed black lines in Fig. 3 represent the field profiles obtained based on the paraxial approximation described in Sec. III, whereas the solid blue lines represent the field profiles obtained using the more rigorous (nonparaxial) theory of Appendix A. The two approaches yield nearly coincident results, consistent with the beam being a quasi-TEM wave. In particular, it is seen in the lower-right panel of Fig. 3 that $n_{ef,h}^2 \approx n_w^2/\zeta_w$, consistent with Eq. (2). In the region where the field intensity is stronger, $n_{ef,h}^2 < 1$, because the dielectric host is a self-defocusing Kerr medium. The envelope of E_y has even parity, whereas the envelopes of E_z and φ_w have odd parity with respect to the coordinate y.

It can be checked that for the example of Fig. 3, the half-power beamwidth (which is roughly determined by the envelope of E_y) is such that $W = 1.06\lambda_0$; thus, it is on the order of the free-space wavelength. As could be expected, the beamwidth depends on the strength of the nonlinear effects, and for greater field intensities (smaller values of k_z), W becomes increasingly smaller and may even become subwavelength. This is illustrated in Fig. 4, where the half-power beamwidth is depicted as a function of the required value of $n_{ef,h}^2$ at the center of the beam. The results of Fig. 4 were obtained based on the nonparaxial approximation. Unfortunately, the condition to have a subwavelength solitons may require unrealistically strong nonlinear effects, associated with a significant depression of $n_{ef,h}^2$ (at least 5%) compared to the case of a linear response.

To understand how the specific geometry of the nanowire material affects the profile of the spatial solitons, I computed the solitons associated $k_z = 0.993k_h$ in a material formed by

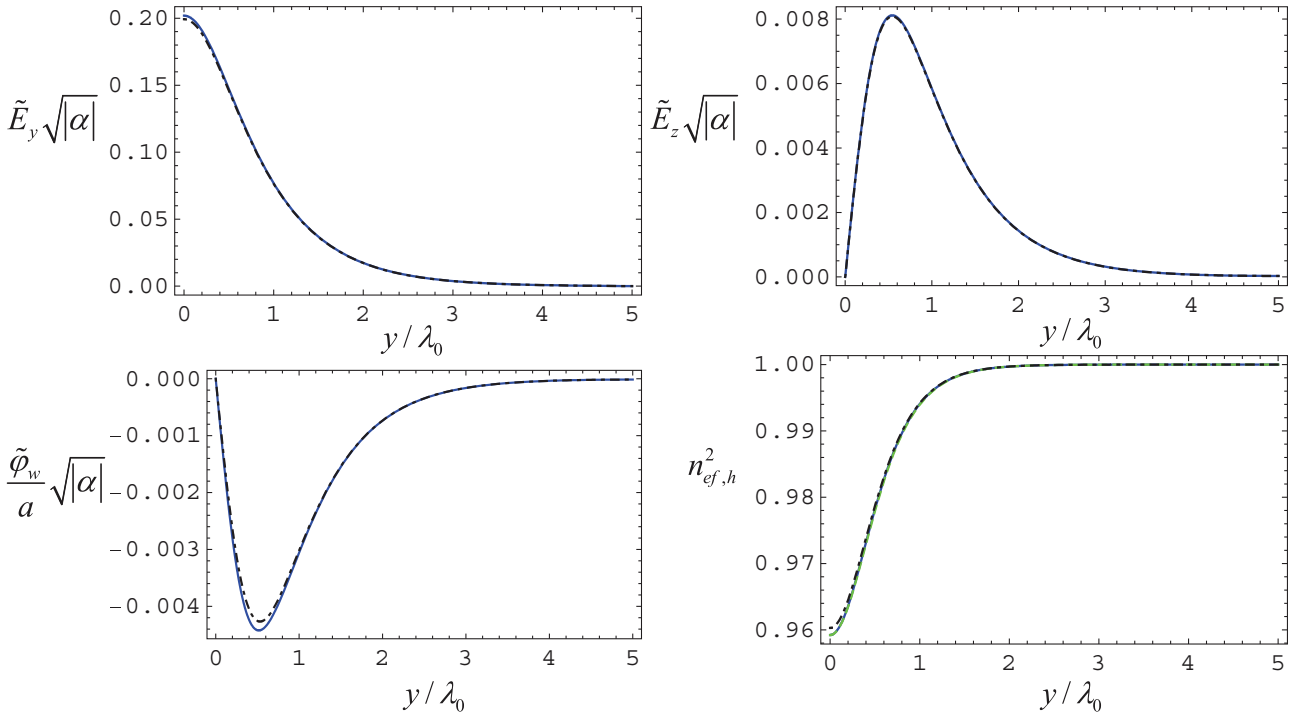

FIG. 3. (Color online) Normalized field profiles ($E_y = \tilde{E}_y(y)e^{ik_z z}$, $E_z = i\,\tilde{E}_z(y)e^{ik_z z}$, and $\varphi_w = \tilde{\varphi}_w(y)e^{ik_z z}$) for a spatial soliton with $k_z = 0.990k_h$ at λ_0=1550 nm in a nanowire material formed by silver wires in a dielectric background with $\varepsilon_h^0 = 1.0\varepsilon_0$, $r_w = 20$ nm, and $r_w/a = 0.1$. Solid blue lines are profiles calculated based on the nonparaxial approximation. Dot-dashed black lines are profiles calculated based on the paraxial approximation. The dashed green line (virtually coincident with the solid blue line) in the lower-right panel represents n_w^2/ζ_w.

an array of silver nanowires embedded in a self-defocusing dielectric, considering different frequencies of operation and different nanowire radii and periods. The results of Fig. 5 indicate that for a fixed value of k_z/k_h, the electric field amplitude required to have the formation of a spatial soliton is nearly independent of r_w,a,λ_0.

In addition, Fig. 5(d) shows that the characteristic spatial width of the soliton depends directly on the degree of hyperbolicity of the dispersion curve of the photonic states in the linear case. Specifically, if for a specific combination of the parameters r_w,a,λ_0 the dispersion curve of the photonic states becomes more hyperbolic, then the beamwidth of the solitary wave becomes larger (Fig. 5(a) and (d)). This result is consistent with the property discussed in Sec. III that in the limit of flat dispersion contours (in case of a PEC metal), the nanowire material can support nondiffracting waves with an arbitrary transverse beamwidth length, even in the limit of vanishingly small nonlinear effects. Because of the plasma-type electric response of the nanowires, the isofrequency contours of the photonic modes become more hyperbolic for shorter wavelengths and very dilute systems (r_w/a very small). As a consequence, in these scenarios, the beamwidth of the spatial solitons tends to increase, as illustrated in Fig. 5(a).

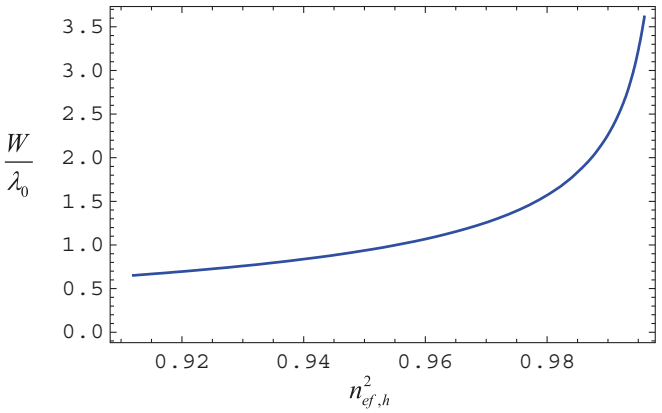

FIG. 4. (Color online) Normalized half-power beamwidth W of the spatial solitons as a function of $n^2_{ef,h}$ at $\lambda_0 = 1550$ nm in a nanowire material formed by silver wires in a dielectric background with $\varepsilon_h^0 = 1.0\varepsilon_0$, $r_w = 20$ nm, and $r_w/a = 0.1$.

V. EFFECT OF LOSS

In the previous sections, the impact of dielectric and metal loss was not taken into account. In order to characterize the characteristic propagation length of the spatial solitons in more realistic scenarios, I next investigate the spatial evolution of the solitary wave in the presence of material loss.

To this end, consider again Eq. (3) with $\mathbf{j}_{\text{ext}} = 0$, $E_x = 0$, and $\partial_x = 0$. It is simple to verify that $\nabla \times \mathbf{E} = F_x\hat{\mathbf{x}}$ with $F_x = \frac{\partial E_z}{\partial y} - \frac{\partial E_y}{\partial z}$. Evidently, F_x is proportional to the x component of the macroscopic magnetic field: $F_x = i\omega\mu_0 H_x$. It is simple to check that Eq. (3) can be rewritten as

$$\frac{\partial F_x}{\partial z} = k_h^2 n_{ef,h}^2 E_y, \tag{7a}$$

$$\frac{\partial \varphi_w}{\partial z} = \frac{\zeta_w}{\beta_p^2}\left[-\frac{\partial F_x}{\partial y} - \left(k_h^2 n_{ef,h}^2 - \frac{\beta_p^2}{\zeta_w}\right)E_z\right], \tag{7b}$$

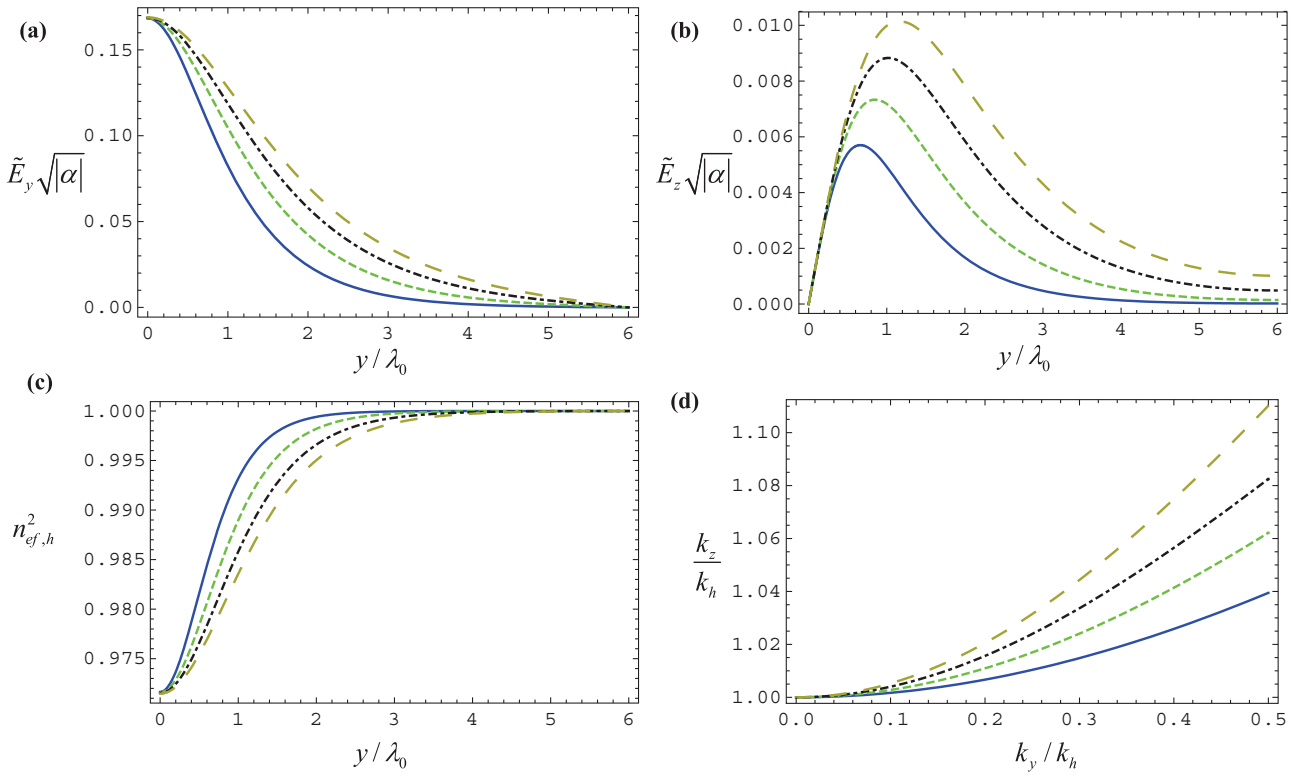

FIG. 5. (Color online) (a) and (b) Normalized field profiles ($E_y = \tilde{E}_y(y)e^{ik_z z}$, $E_z = i\,\tilde{E}_z(y)e^{ik_z z}$) for a spatial soliton with $k_z = 0.993k_h$ in a material formed by silver nanowires in a dielectric background with $\varepsilon_h^0 = 1.0\varepsilon_0$. (c) Profile of the index of refraction associated with the spatial soliton. (d) Dispersion of the photonic states associated with the extraordinary (quasi-TEM) wave in case of a linear host with $n^2_{ef,h} = n^2_w/\zeta_w = 1.0$. Solid blue lines are $r_w = 20\,\text{nm}$, $a = 200\,\text{nm}$, and $\lambda_0 = 1550\,\text{nm}$; dashed green lines are $r_w = 20\,\text{nm}$, $a = 200\,\text{nm}$, and $\lambda_0 = 1300\,\text{nm}$; dot-dashed black lines are $r_w = 20\,\text{nm}$, $a = 267\,\text{nm}$, and $\lambda_0 = 1550\,\text{nm}$; and long-dashed dark yellow lines are $r_w = 14\,\text{nm}$, $a = 200\,\text{nm}$, and $\lambda_0 = 1550\,\text{nm}$.

$$\frac{\partial E_z}{\partial z} = \left(k_h^2\zeta_w n^2_{ef,h} + \frac{\partial^2}{\partial z^2}\right)\varphi_w, \tag{7c}$$

$$\frac{\partial E_y}{\partial z} = \frac{\partial E_z}{\partial y} - F_x. \tag{7d}$$

Since the dominant component of the solitary wave is E_y, we can assume that $\frac{\partial}{\partial z} \to ik_{z0}$ when the operator ∂_z acts over φ_w and E_z. Hence, Eqs. (7b) and (7c) yield

$$ik_{z0}\varphi_w = \frac{\zeta_w}{\beta_p^2}\left[-\frac{\partial F_x}{\partial y} - \left(k_h^2 n^2_{ef,h} - \frac{\beta_p^2}{\zeta_w}\right)E_z\right], \tag{8a}$$

$$ik_{z0}E_z = \left(k_h^2\zeta_w n^2_{ef,h} - k_{z0}^2\right)\varphi_w. \tag{8b}$$

Substituting Eq. (8a) into (8b), it is found that

$$\left(1 - \frac{\beta_p^2}{k_h^2\zeta_w n^2_{ef,h} - k_{z0}^2}\right)k_h^2 n^2_{ef,h}E_z = -\frac{\partial F_x}{\partial y}. \tag{9}$$

Substituting this result into Eq. (7d), it follows that

$$\frac{\partial E_y}{\partial z} = -\frac{\partial}{\partial y}\left[\left(1 - \frac{\beta_p^2}{k_h^2\zeta_w n^2_{ef,h} - k_{z0}^2}\right)^{-1}\frac{1}{k_h^2 n^2_{ef,h}}\frac{\partial F_x}{\partial y}\right] - F_x. \tag{10}$$

Because $n^2_{ef,h}$ is expected to vary relatively slowly in space, it is possible to neglect its derivatives with respect to y and z. Differentiating both members of Eq. (10) with respect to z and using Eq. (7a), it follows after some simplifications that

$$\frac{\partial^2 E_y}{\partial z^2} + k_h^2 n^2_{ef,h}E_y = -\left(1 - \frac{\beta_p^2}{k_h^2\zeta_w n^2_{ef,h} - k_{z0}^2}\right)^{-1}\frac{\partial^2 E_y}{\partial y^2}. \tag{11}$$

Writing $E_y = \tilde{E}_y(y,z)e^{ik_{z0}z}$ and using the standard paraxial approximation $\frac{\partial^2}{\partial z^2} \to 2ik_{z0}\frac{\partial}{\partial z} - k_{z0}^2$, reveals an equation that enables calculation of the spatial evolution of the field envelope $\tilde{E}_y(y,z)$ along the direction of propagation:

$$2ik_{z0}\frac{\partial \tilde{E}_y}{\partial z} = -\left(1 - \frac{\beta_p^2}{k_h^2\zeta_w n^2_{ef,h} - k_{z0}^2}\right)^{-1}\frac{\partial^2 \tilde{E}_y}{\partial y^2} - \left(k_h^2 n^2_{ef,h} - k_{z0}^2\right)\tilde{E}_y. \tag{12}$$

Specifically, the spatial evolution is determined assuming that $\tilde{E}_y(y,z=0)$ is the profile of the spatial soliton associated with $k_z = k_{z0}$ in the lossless case, calculated as explained in Sec. III. Then, the evolution of $\tilde{E}_y(y,z)$ is determined by solving Eq. (12), including the effect of metal loss in the parameter ζ_w and the effect of dielectric loss in $k_h = \omega\sqrt{\varepsilon_h^0\mu_0}$ and using the boundary conditions $\tilde{E}_y(\pm y_{\max},z) = 0$, where $y_{\max} \gg W$ is and W is the beamwidth of the spatial soliton. In the calculations, the effect of loss in silver was modeled

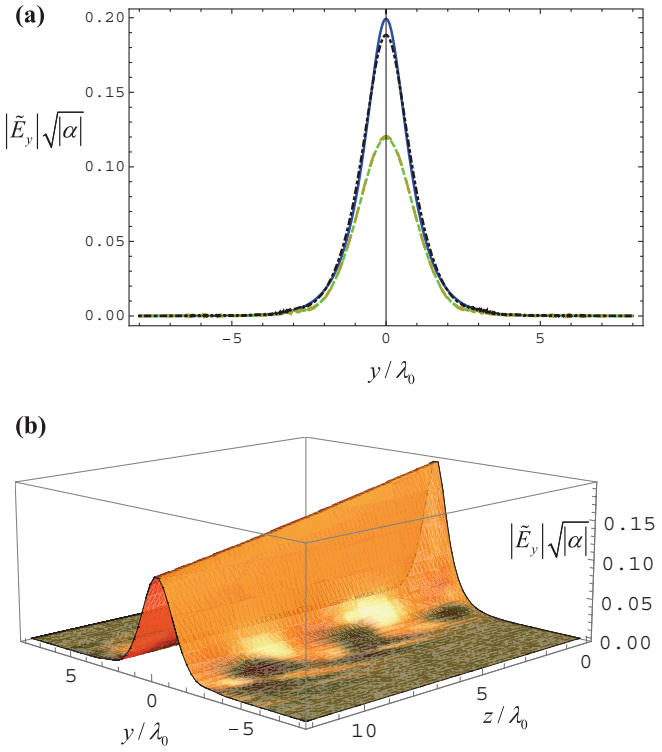

FIG. 6. (Color online) Normalized field profile of a spatial soliton with $k_z = 0.990k_h$ at $\lambda_0 = 1550$ nm in a nanowire material formed by silver wires in a dielectric background with $\mathrm{Re}\{\varepsilon_h^0\} = 1.0\varepsilon_0$, $r_w = 20$ nm, and $r_w/a = 0.1$ after a propagation distance of $12\lambda_0$. (a) Solid blue line: Loss effect is neglected. Green dashed line: Effect loss in the silver nanowires and host medium is taken into account. Black dashed line: Only loss in the metal is taken into account. Dark yellow long-dashed line (practically coincident with the green line): Only loss in the host dielectric is taken into account. (b) Profile of the spatial soliton when loss is considered in both the dielectric and the silver. The host medium is modeled as a lossy dielectric with the loss tangent $\tan\delta = 0.01$.

by assuming that the collision frequency associated with the Drude model is 4.35 THz.[25]

I calculated the amplitude of the field envelope profile for the case of a spatial soliton associated with $k_z = 0.990k_h$ at λ_0=1550 nm, which corresponds to the same example as in Fig. 3. The normalized calculated $|\tilde{E}_y|$, after a propagating distance of $12\lambda_0$, is shown in Fig. 6(a) for the lossless case (solid blue line) and several lossy cases. As shown by the (black) dashed curve, the effect of metal loss is relatively weak, and the reduction in the soliton amplitude is almost insignificant. This is explained in part by the relatively weak loss of silver in the infrared regime. However, the main reason for the weak sensitivity to loss in the metal is that the solitary wave is a quasi-TEM beam (see Fig. 3); consequently, it interacts relatively weakly with the metallic wires, being the electric field mostly concentrated in the dielectric host. Consistent with this observation, it is seen in Fig. 6(a) (dark yellow long-dashed curve) that the amplitude of the soliton is notably affected by the dielectric loss in the self-defocusing host dielectric. The green dashed curve in Fig. 6(a), calculated for the case in which metal and dielectric loss are both considered, further supports that the impact of metal loss is negligible compared to dielectric loss.

Figure 6(b) reports the detailed spatial evolution of the solitary wave when loss is considered in both the dielectric and the silver. The numerical simulations, based on Eq. (12), also indicate that the profile of the solitary waves is stable to perturbations. The considered spatial solitons cannot, as a result of some perturbation, be collapsed into an increasingly narrower beam, because at a scale length on the order of the period a, the effective medium approximation ceases to work. In particular, a beam more localized than the period of the nanowire material effectively sees the "self-defocusing" host. Thus, the granularity of the lattice prevents the concentration of the solitary beam in a scale length smaller than the period a.

VI. CONCLUSION

Based on an effective medium approximation, I characterized the spatial solitons supported by metallic nanowire arrays embedded in a Kerr-type medium. I studied the physical requirements for the formation of spatial solitons in nanowires structures. Taking into account the dynamics of the isofrequency surfaces of the photonic states in the nanowire material with respect to intensity of the electromagnetic field, it was shown that within the continuous medium approximation, spatial solitons are supported only when the host dielectric is a self-defocusing material. It was demonstrated that, for sufficiently strong electric field amplitude, the spatial solitons may become subwavelength and that the main decay channel for the solitons is related to the loss in the dielectric, being the metallic loss comparatively less relevant. The developed theory provides a simple means to characterize and analyze the formation and propagation of optical lattice solitons in metallic nanowire structures.

ACKNOWLEDGMENTS

The author gratefully acknowledges fruitful discussions with Fabio Biancalana and Andrea Marini. This work is supported in part by Fundação para Ciência e a Tecnologia under Project No. PTDC/EEI-TEL/2764/2012.

APPENDIX A

Here, the formalism used to determine the spatial solitons is developed. First, consider the more general case (nonparaxial approach) wherein only the contribution of $|E_z|^2$ to n_w^2 and $n_{ef,h}^2$ is neglected so that

$$n_w^2 \approx \zeta_w\left[1 + \alpha\left(\mathbf{E}_t^* \cdot \mathbf{E}_t + \tilde{B}\,\beta_p^2 \varphi_w \varphi_w^*\right)\right], \tag{A1a}$$

$$n_{ef,h}^2 \approx 1 + \alpha\left(\mathbf{E}_t^* \cdot \mathbf{E}_t + \beta_p^2 \varphi_w \varphi_w^*\right). \tag{A1b}$$

We want to solve the nonlinear system in Eq. (1) based on the preceding approximate formulas for n_w^2 and $n_{ef,h}^2$ and using the exact formula of $\tilde{\mathbf{Y}}$. We are interested in solitons such that the dependence on z of $(\mathbf{E}, \varphi_w)$ is of the form $e^{ik_z z}$, $E_x = 0$, and $\partial_x = 0$ (the wave propagation and the electric field are in the yoz plane). In this case, Eq. (1a) with $\mathbf{j}_{\mathrm{ext}} = 0$

can be spelled out as follows:

$$ik_z\frac{\partial E_z}{\partial y} = -\left(k_z^2 - k_h^2 n_{ef,h}^2\right)E_y + \beta_p^2 k_h^2 \tilde{Y}_y \varphi_w, \tag{A2a}$$

$$-\frac{\partial^2 E_z}{\partial y^2} + ik_z\frac{\partial E_y}{\partial y} = \left(k_h^2 n_{ef,h}^2 - \frac{\beta_p^2}{\zeta_w}\right)E_z + \frac{\beta_p^2}{\zeta_w} ik_z \varphi_w, \tag{A2b}$$

with $\tilde{Y}_y = \frac{\alpha}{2}(\varphi_w E_y^* + \varphi_w^* E_y)$. On the other hand, using Eq. (1b), it is possible to obtain an explicit expression for E_z in terms of $\mathbf{E}_t$ and φ_w:

$$E_z = \left[\left(k_h^2 n_w^2 - k_z^2\right)\varphi_w + \zeta_w k_h^2 \tilde{\mathbf{Y}} \cdot \mathbf{E}_t\right]/(ik_z). \tag{A3}$$

It is proven in Appendix B that by substituting this result into Eq. (A2), it is possible to eliminate E_z and obtain a nonlinear system for E_y and φ_w. We are interested in spatial solitons such that E_y and φ_w are in phase. Specifically, it is assumed that $E_y = \tilde{E}_y(y)e^{ik_z z}$ and $\varphi_w = \tilde{\varphi}_w(y)e^{ik_z z}$, with the envelopes $\tilde{E}_y$ and $\tilde{\varphi}_w$ real valued. In these circumstances, E_y and φ_w satisfy the first-order partial-nonlinear system (see Appendix B)

$$\mathbf{A}\cdot\mathbf{y} = \mathbf{b}, \tag{A4}$$

where $\mathbf{y} = (\frac{\partial \varphi_w}{\partial y}\ \frac{\partial E_y}{\partial y})^T$ and the 2×2 matrix $\mathbf{A} = [a_{i,j}]$ has the elements

$$a_{11} = k_h^2 n_w^2 - k_z^2 + \alpha\zeta_w k_h^2 E_y E_y^* + 2\alpha\zeta_w k_h^2 \tilde{B}\,\beta_p^2 \varphi_w \varphi_w^*, \tag{A5a}$$

$$a_{12} = \zeta_w k_h^2 \tilde{Y}_y + 3\alpha\zeta_w k_h^2 E_y \varphi_w^*, \tag{A5b}$$

$$a_{21} = -\left(\beta_p^2 \tilde{Y}_y + 3\alpha\beta_p^2 E_y \varphi_w^*\right), \tag{A5c}$$

$$a_{22} = -\left(n_{ef,h}^2 + 2\alpha E_y E_y^* + \alpha\beta_p^2 \varphi_w \varphi_w^*\right). \tag{A5d}$$

Vector $\mathbf{b}$ in the right-hand side of Eq. (A4) is given by

$$\mathbf{b} = \begin{pmatrix} -\left(k_z^2 - k_h^2 n_{ef,h}^2\right)E_y + \beta_p^2 k_h^2 \tilde{Y}_y \varphi_w \\ \left(k_h^2 n_{ef,h}^2 \zeta_w - \beta_p^2\right)\tilde{Y}_y E_y + \left[\left(k_h^2 n_w^2 - k_z^2\right)n_{ef,h}^2 - \frac{\beta_p^2}{\zeta_w} n_w^2\right]\varphi_w \end{pmatrix}. \tag{A6}$$

The reason we look for spatial solitons such that E_y and φ_w are in phase is that in such circumstances, it follows from Eq. (A3) that E_y and E_z are in quadrature in the limit of negligible material loss. The n_w^2, ζ_w, and $\tilde{Y}_y$ are real valued when loss is negligible and E_y and φ_w are in phase. For a plane wave natural mode in the uniaxial wire medium, it can be proven that in the linear case ($\alpha = 0$) and in the limit of negligible loss, the phase difference between E_y and E_z (with $E_x = 0$) is the same as the phase difference between k_y and k_z, where $\mathbf{k} = (0, k_y, k_z)$ is the wave vector of the plane wave.[17,18] Thus, when E_y and E_z are in quadrature, the wave vector components k_y and k_z are also in quadrature. In particular, when k_z is real valued, the natural mode has an exponential-type variation along the y direction. This suggests that solutions of Eq. (A2) with E_y and E_z in quadrature and a variation along z of the form $e^{ik_z z}$ with k_z real valued may be associated with waves that decay exponentially when $y \to \pm\infty$ and propagate along z, which is the desired behavior for the spatial solitons.

In the paraxial approximation, only the contributions to the nonlinear dynamics arising from terms of the form $E_y E_y^*$ should be retained. Hence, within this approximation, we should set equal to zero terms of form $\tilde{Y}_y$, $\varphi_w\varphi_w^*$, and $E_y\varphi_w^*$ in Eqs. (A5) and (A6). It can be readily checked that this yields the nonlinear system of Eqs. (3a) and (3b).

APPENDIX B

To obtain the nonlinear differential system in Eq. (A4), first calculate $\frac{\partial^2 E_z}{\partial y^2} = \frac{\partial}{\partial y}\frac{\partial E_z}{\partial y}$ in the left-hand side of Eq. (A2b) with the help of the explicit formula for $\frac{\partial E_z}{\partial y}$, given by Eq. (A2a). This gives

$$\frac{\partial}{\partial y}\left[k_h^2 n_{ef,h}^2 E_y + \beta_p^2 k_h^2 \tilde{Y}_y \varphi_w\right] = (-ik_z)\left(k_h^2 n_{ef,h}^2 - \frac{\beta_p^2}{\zeta_w}\right)E_z + \frac{\beta_p^2}{\zeta_w} k_z^2 \varphi_w. \tag{B1}$$

By substituting Eq. (A3) into Eqs. (A2a) and (B1), it is found after straightforward simplifications that

$$\frac{\partial}{\partial y}\left[\left(k_h^2 n_w^2 - k_z^2\right)\varphi_w + \zeta_w k_h^2 \tilde{Y}_y E_y\right] = b_1, \tag{B2a}$$

$$-\frac{\partial}{\partial y}\left[n_{ef,h}^2 E_y + \beta_p^2 \tilde{Y}_y \varphi_w\right] = b_2, \tag{B2b}$$

where b_1 and b_2 are such that $\mathbf{b} = (b_1 b_2)^T$ is given by Eq. (A6). Next, we calculate explicitly the derivatives in the left-hand side of Eq. (B2) with the help of $\tilde{Y}_y = \frac{\alpha}{2}(\varphi_w E_y^* + \varphi_w^* E_y)$ and of the formulas for n_w^2 and $n_{ef,h}^2$ (Eqs. (A1a) and (A1b)). This yields a nonlinear system that can be written in the matrix form

$$\mathbf{M}\cdot\mathbf{x} = \mathbf{b}, \tag{B3}$$

with $\mathbf{x} = (\frac{\partial \varphi_w}{\partial y}\ \frac{\partial \varphi_w^*}{\partial y}\ \frac{\partial E_y}{\partial y}\ \frac{\partial E_y^*}{\partial y})^T$. The 2×4 matrix $\mathbf{M} = [m_{i,j}]$ has the following elements:

$$m_{11} = k_h^2 n_w^2 - k_z^2 + \frac{\alpha}{2}\zeta_w k_h^2 E_y E_y^* + \alpha\zeta_w k_h^2 \tilde{B}\,\beta_p^2 \varphi_w \varphi_w^* \tag{B4a}$$

$$m_{12} = \alpha\zeta_w k_h^2 \tilde{B}\,\beta_p^2 \varphi_w^2 + \frac{\alpha}{2}\zeta_w k_h^2 E_y^2 \tag{B4b}$$

$$m_{13} = \zeta_w k_h^2 \tilde{Y}_y + \frac{\alpha}{2}\zeta_w k_h^2 E_y \varphi_w^* + \alpha\zeta_w k_h^2 \varphi_w E_y^* \tag{B4c}$$

$$m_{14} = \frac{3}{2}\alpha\zeta_w k_h^2 E_y \varphi_w \tag{B4d}$$

$$m_{21} = -\left(\beta_p^2 \tilde{Y}_y + \alpha\beta_p^2 E_y \varphi_w^* + \frac{\alpha}{2}\beta_p^2 \varphi_w E_y^*\right) \tag{B4e}$$

$$m_{22} = -\frac{3}{2}\alpha\beta_p^2 \varphi_w E_y \tag{B4f}$$

$$m_{23} = -\left(n_{ef,h}^2 + \alpha E_y E_y^* + \frac{\alpha}{2}\beta_p^2 \varphi_w \varphi_w^*\right) \tag{B4g}$$

$$m_{24} = -\alpha\left(E_y^2 + \frac{1}{2}\beta_p^2 \varphi_w^2\right) \tag{B4h}$$

If E_y and φ_w are assumed to be in phase, it is straightforward to check that the system in Eq. (B3) reduces to Eq. (A4).

*Corresponding author: mario.silveirinha@co.it.pt

[1] C. R. Simovski, P. A. Belov, A. V. Atrashchenko, and Y. S. Kivshar, Adv. Mater. **24**, 4229 (2012).

[2] P. A. Belov, Y. Hao, and S. Sudhakaran, Phys. Rev. B **73**, 033108 (2006).

[3] P. Ikonen, C. Simovski, S. Tretyakov, P. Belov, and Y. Hao, Appl. Phys. Lett. **91**, 104102 (2007).

[4] G. Shvets, S. Trendafilov, J. B. Pendry, and A. Sarychev, Phys. Rev. Lett. **99**, 053903 (2007).

[5] N. N. Akhmediev, Opt. Quant. Elect. **30**, 535 (1998).

[6] Y. S. Kivshar and G. P. Agrawal, *Optical Solitons* (Academic Press, San Diego, CA, 2003).

[7] Y. Liu, G. Bartal, D. A. Genov, and X. Zhang, Phys. Rev. Lett. **99**, 153901 (2007).

[8] F. Ye, D. Mihalache, B. Hu, and N. C. Panoiu, Phys. Rev. Lett. **104**, 106802 (2010).

[9] J.-Y. Yan, L. Li, and J. Xiao, Optic. Express **20**, 1945 (2012).

[10] A. I. Maimistov, I. R. Gabitov, and A. O. Korotkevich, Quant. Electron. **37**, 549 (2007).

[11] I. R. Gabitov, A. O. Korotkevich, A. I. Maimistov, and J. B. McMahon, Appl. Phys. Mater. Sci. Process. **89**, 277 (2007).

[12] N. M. Litchinitser, I. R. Gabitov, and A. I. Maimistov, Phys. Rev. Lett. **99**, 113902 (2007).

[13] I. R. Gabitov, A. O. Korotkevich, A. I. Maimistov, and J. B. McMahon, in *Dissipative Solitons: From Optics to Biology and Medicine*, edited by N. N. Akhmediev and A. Ankiewicz, Vol. 751 (Springer, Berlin, Heidelberg, 2008).

[14] F. Ye, D. Mihalache, B. Hu, and N. C. Panoiu, Opt. Lett. **36**, 1179 (2011).

[15] Y. Kou, F. Ye, and X. Chen, Phys. Rev. A **84**, 033855 (2011).

[16] M. G. Silveirinha, Phys. Rev. B **87**, 165127 (2013).

[17] P. A. Belov, R. Marqués, S. I. Maslovski, I. S. Nefedov, M. Silveirinha, C. R. Simovski, and S. A. Tretyakov, Phys. Rev. B **67**, 113103 (2003).

[18] M. G. Silveirinha, Phys. Rev. E **73**, 046612 (2006).

[19] S. I. Maslovski and M. G. Silveirinha, Phys. Rev. B **80**, 245101 (2009).

[20] M. G. Silveirinha, P. A. Belov, and C. R. Simovski, Phys. Rev. B **75**, 035108 (2007).

[21] J. Yao, Z. Liu, Y. Liu, Y. Wang, C. Sun, G. Bartal, A. M. Stacy, and X. Zhang, Science **321**, 930 (2008).

[22] M. A. Noginov, H. Li, Y. A. Barnakov, D. Dryden, G. Nataraj, G. Zhu, C. E. Bonner, M. Mayy, Z. Jacob, and E. E. Narimanov, Opt. Lett. **35**, 1863 (2010).

[23] A. N. Poddubny, P. A. Belov, and Y. S. Kivshar, Phys. Rev. A **84**, 023807 (2011).

[24] H. N. S. Krishnamoorthy, Z. Jacob, E. Narimanov, I. Kretzschma, and V. M. Menon, Science **336**, 205 (2012).

[25] M. A. Ordal, R. J. Bell, R. W. Alexander Jr., L. L. Long, and M. R. Querry, Appl. Opt. **24**, 4493 (1985).

[26] W. Chen and D. L. Mills, Phys. Rev. Lett. **58**, 160 (1987).

[27] D. Mandelik, R. Morandotti, J. S. Aitchison, and Y. Silberberg, Phys. Rev. Lett. **92**, 093904 (2004).

[28] S. Longhi, Wave. Random Complex Media **15**, 119 (2005).

[29] M. G. Silveirinha, P. A. Belov, and C. R. Simovski, Opt. Lett. **33**, 1726 (2008).